

Titolo

ANALYSIS OF EXPERIMENTS IN TAPIRO AND STUDY OF THE EFFECTS OF NUCLEAR DATA IN THE SIMULATIONS

Descrittori

Tipologia del documento: Rapporto Tecnico

Collocazione contrattuale: Accordo di programma ENEA-MSE su sicurezza nucleare e reattori di IV generazione

Argomenti trattati: Generation IV reactors

Sommario

Il reattore TAPIRO è un impianto sperimentale che può fornire importanti informazioni sulla qualità dei dati nucleari utilizzati per la fisica dei reattori. In particolare, la presenza di una grande quantità di rame nel riflettore, consente di qualificare l'adeguatezza dei dati esistenti per questo materiale in varie librerie di dati di base. In questo lavoro, il codice Serpent è usato per simulare i tassi di reazione che sono stati misurati in una campagna sperimentale condotta in passato. Il confronto quantifica le differenze nei risultati ottenuti utilizzando le librerie JEFF-3.1.1 e ENDF/B-VIII.

The TAPIRO reactor is an experimental facility that may provide important information on the quality of nuclear data used for reactor physics evaluations. In particular, the presence of a large quantity of copper in the reflector, allows to qualify the adequateness of the existing data for this material in various libraries. In this work, the Serpent code is used to simulate reaction rates that were measured in an experimental campaign carried out in the past. The comparison quantifies the differences in the results obtained using JEFF-3.1.1 and ENDF/B-VIII libraries

Note

Autori: M. Carta, V. Fabrizio (ENEA)

D. Caron, C. Di Gesare, S. Dulla, P. Ravetto (Politecnico di Torino)

Copia n.
In carico a:

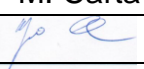
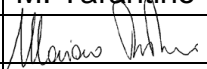
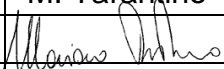

2			NOME			
			FIRMA			
1			NOME			
			FIRMA			
0	EMISSIONE	28/11/2018	NOME	M. Carta	M. Tarantino	M. Tarantino
			FIRMA			
REV.	DESCRIZIONE	DATA		REDAZIONE	CONVALIDA	APPROVAZIONE

TABLE OF CONTENTS

1	INTRODUCTION AND PREVIOUS WORK	3
2	THE TAPIRO REACTOR.....	4
3	THE TAPIRO SERPENT MODEL AND NUCLEAR DATA.....	5
4	COMPARISON OF NUCLEAR DATA LIBRARIES.....	8
4.1	Copper cross section behavior in JEFF-3.1.1 vs. ENDF/B-VIII.....	8
4.2	Effect of cross section data on the fission rate Monte Carlo estimations	10
5	CONCLUSIONS	16
6	LIST OF REFERENCES	16

 Ricerca Sistema Elettrico	Sigla di identificazione	Rev.	Distrib.	Pag.	di
	ADPFISS – LP2 – 157	0	L	3	17

1 INTRODUCTION AND PREVIOUS WORK

The sustainable use of nuclear fission energy requires the development of technologies for a reliable fuel cycle and a safe management of radioactive waste. In particular, the main hazard in spent nuclear fuel is associated to a few chemical elements, e.g. plutonium and Minor Actinides (MAs). It is then necessary to address the appropriate management of these elements, in particular in the perspective of their transmutation in a nuclear system. However, due to a lack of experimental data, and thus large uncertainties on MA nuclear properties, it remains difficult to establish a detailed and reliable design for a transmutation system.

The issue regarding MA nuclear data assessment has been pointed out by several NEA and IAEA Working Groups, recommending the development of new experimental campaigns involving both integral and differential measurements for MA. In the framework of the NEA Expert Group on Integral Experiments for Minor Actinide Management [1] a joint collaboration between ENEA (Italian National Agency for New Technologies, Energy and Sustainable Economic Development) and CEA (French Alternative Energies and Atomic Energy Commission) was established with the aim to study the feasibility of a MA irradiation campaign in the TAPIRO fast neutron source research reactor, located at the ENEA Casaccia center near Rome [2]. A previous campaign, performed during the 80's in collaboration with SCK-CEN Mol (Belgium), allowed a thorough neutronic characterization of the reactor, showing that TAPIRO can provide a wide set of neutron sources with different energy spectra, thus allowing a variety of irradiation configurations.

The activity for the neutronic characterization of TAPIRO has been re-established in recent years [3-4], focusing the attention on the possible irradiation, in various experimental set-ups, of some CEA samples loaded with different contents of MA, coming from the French experimental campaigns OSMOSE and AMSTRAMGRAM. The results of these future measurements could be fruitfully employed to improve the available nuclear data by an adjustment procedure [5]. In particular, a simulation activity on the TAPIRO reactor adopting both deterministic (ERANOS [6]) and stochastic (MCNP [7] and Serpent [8]) computational tools was performed [9-10], with the objective of reproducing the reaction rates of some specific experimental samples as measured in the SCK-CEN campaign. This work assessed the suitability of such tools for the neutronic description of TAPIRO, accounting for the unavoidable approximation in geometry and energy treatment associated to a transport calculation. Moreover, the neutronic relevance of the copper reflector in affecting the experimental measurements has been preliminarily tackled, by evaluating the MA reaction rate sensitivity due to a 2% copper density reduction in the whole TAPIRO reflector. These early results showed the importance of the correct modelization of the TAPIRO reflector, both in terms of geometrical representation and nuclear data adopted.

In the present work, the issue associated to the relevance of the nuclear data in correctly simulating the TAPIRO reactor is studied, by comparing different libraries available. In particular, the experimental reaction rates as studied in [9] are considered, and a Serpent Monte Carlo model of TAPIRO is employed, in combination with three different nuclear data sets: the original JEFF-3.1.1 library [11]; an upgraded version of the former with new nuclear data for copper isotopes based on the new ENDF/B-VIII.beta5 library [12-13]; a new library based entirely on ENDF/B-VIII.beta5. The differences among the three different data sets, as well as the resulting effect of the reaction rates observed, are discussed.

2 THE TAPIRO REACTOR

The TAPIRO reactor is a research reactor, characterized by a compact design and small dimensions. The reactor core is a cylinder made of highly enriched metallic uranium (93.5% enrichment), with a cylindrical reflector made of copper and a spherical concrete shielding. Experimental channels penetrate the shielding material and partially the reflector and the core (see Figs. 1 and 2). The main characteristics of TAPIRO, including cooling and control systems, can be found in refs. [2,9].

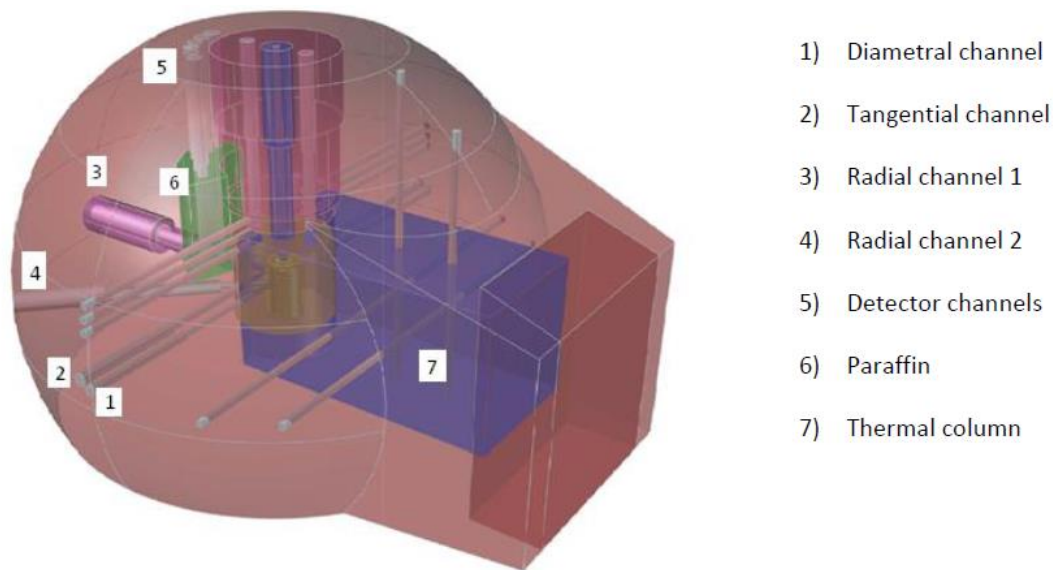


Figure 1 - Irradiation facilities of TAPIRO [2].

The reflector is divided in two regions (inner and outer reflector) both made of natural copper; the inner region is more heterogeneous, due to the presence of the cavities for the control rods and the helium coolant channel [2]. The reactor is able to provide neutron spectra with variable hardness and it reveals a good spherical symmetry of the neutron flux. Therefore, TAPIRO is a versatile device for many applications: validation of calculation codes for generation IV reactors design; study of fast neutron material damage; qualification and tests of innovative detectors. The large quantity of copper in the reactor makes also experiments in TAPIRO very interesting for the study of the neutronics in presence of such material, an issue of relevance also in other nuclear systems, e.g. fusion machines.

During the ENEA-SCK·CEN experimental campaign [14], aiming at the neutronic characterization of the TAPIRO reactor, a large set of reaction rate measurements was performed, covering the entire energy range of practical interest (from 100 eV to 10 MeV). The experimental measurements were carried out using both miniature fission chambers and activation detectors moved inside the different channels at different positions. For each nuclide a different number of measurements have been executed, at different distances from the core.

Starting from this huge set of experimental data, the collaborative work between ENEA and Politecnico di Torino has been focused on the measurements of the fission rates realized along the Radial Channel 1 (RC1) for four selected isotopes: Np-237, U-238, U-235 and Pu-239. The deterministic and stochastic simulations performed showed in general acceptable agreements with experiments, leaving some open issues on both the correct geometrical representation of TAPIRO in the Monte Carlo model and on the role of nuclear data, in particular regarding the material constituting the reflector.

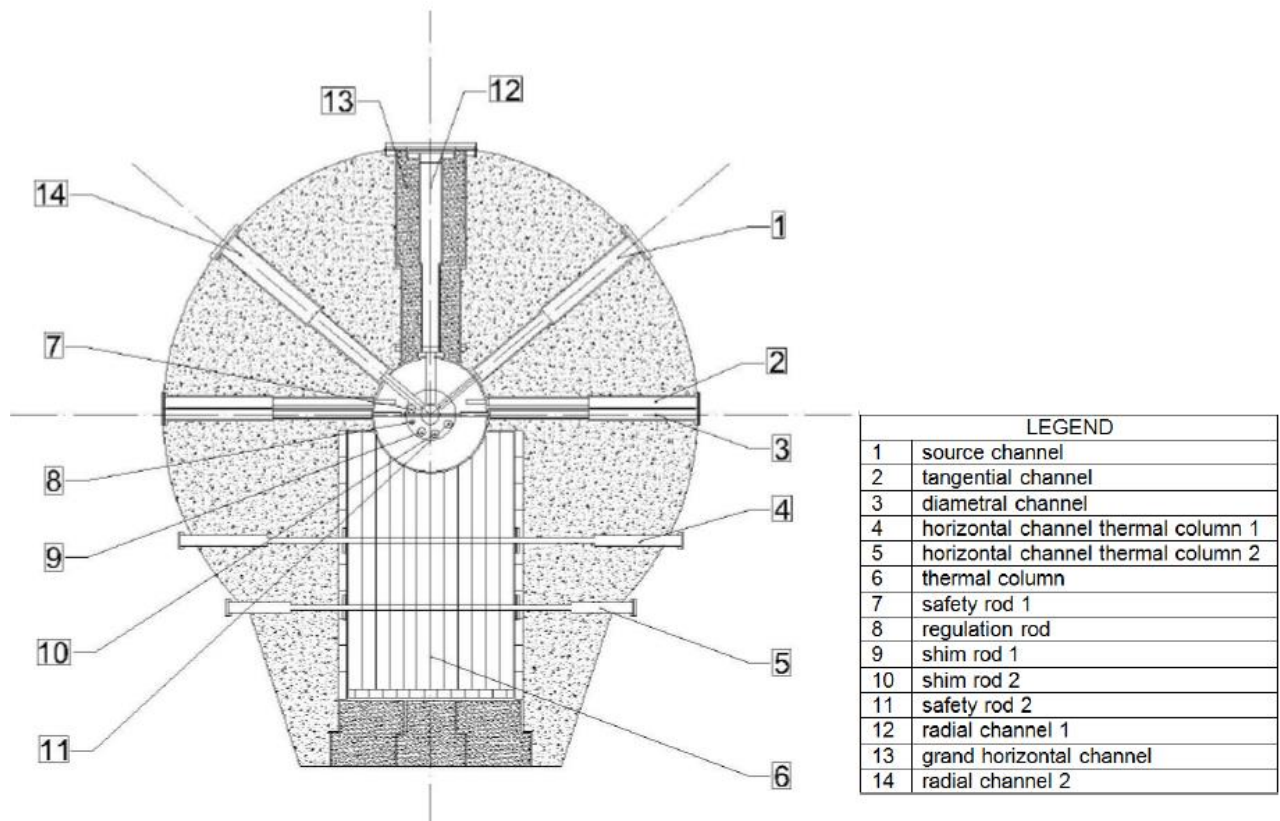


Figure 2 - Section of the reactor parallel to the floor of the reactor room at 100 cm height [2].

3 THE TAPIRO SERPENT MODEL AND NUCLEAR DATA

In [9] a model of the TAPIRO reactor has been implemented in the Serpent Monte Carlo code (version 1.1.19) [8], properly devised to describe the configuration of the reactor during the experimental campaign. The model includes: the core, the primary circuit for the core cooling, the inner and outer reflectors, the diametral, tangential and radial channels and the shielding. The irradiation channels not involved in the measurements are closed by a plug made of the surrounding material (copper/concrete). The steel sleeves encasing the channels are not modelled, due to a limitation of the geometry capabilities of the version of the code

used. A sketch of the core and reactor geometry implemented in Serpent is given in Figs. 3 and 4.

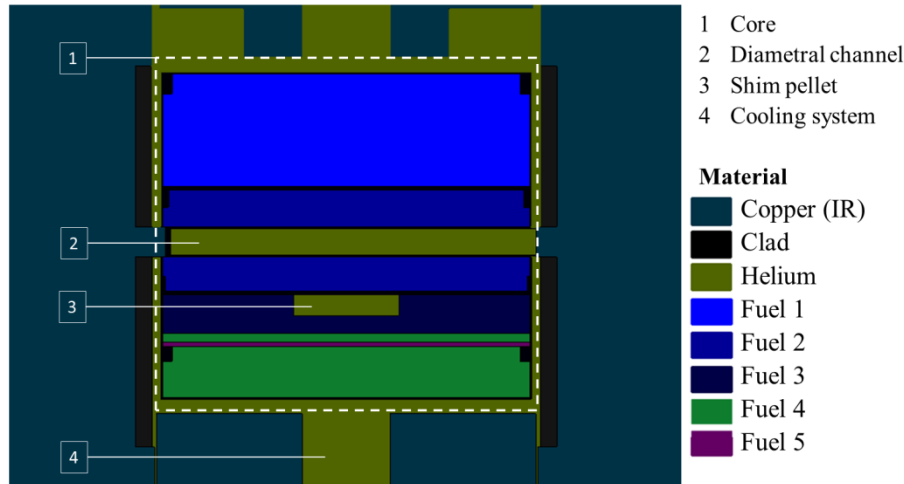


Figure 3 - Serpent model of the TAPIRO core: yz-section at $x=0$.

The RC1 has a square access groove of 0.5 mm side that bores the centre of the plug for the whole length of the channel, allowing the insertion of the miniature fission chambers. In the Monte Carlo code, the access groove is simulated as cylindrical and with a larger size, to reduce the computational time and improve the statistical convergence [9]. Experimental measurements are carried out placing the fission chambers on a copper insert that fills half of the access groove cross section. Moving the copper insert along the access groove axis, the fission chamber can record the fission rate in selected points. In Fig. 5 the model of RC1 is given, with the copper plug in a specific position. To simulate the complete set of measurements for all the isotopes and positions along the channel, a simplified approach has been adopted, collecting all the data in a unique simulation with a fixed position of the copper plug. This approach is acceptable considering the small dimension of the real fission chambers and of the channel itself, that allow to exclude mutual influence. The fission rates are evaluated using virtual detectors with a finite volume filled by the desired material; the dimension of the detectors is large if compared to the size of the real miniature fission chamber, to enhance the statistics. However, such volume is defined in order to be contained in the access groove.

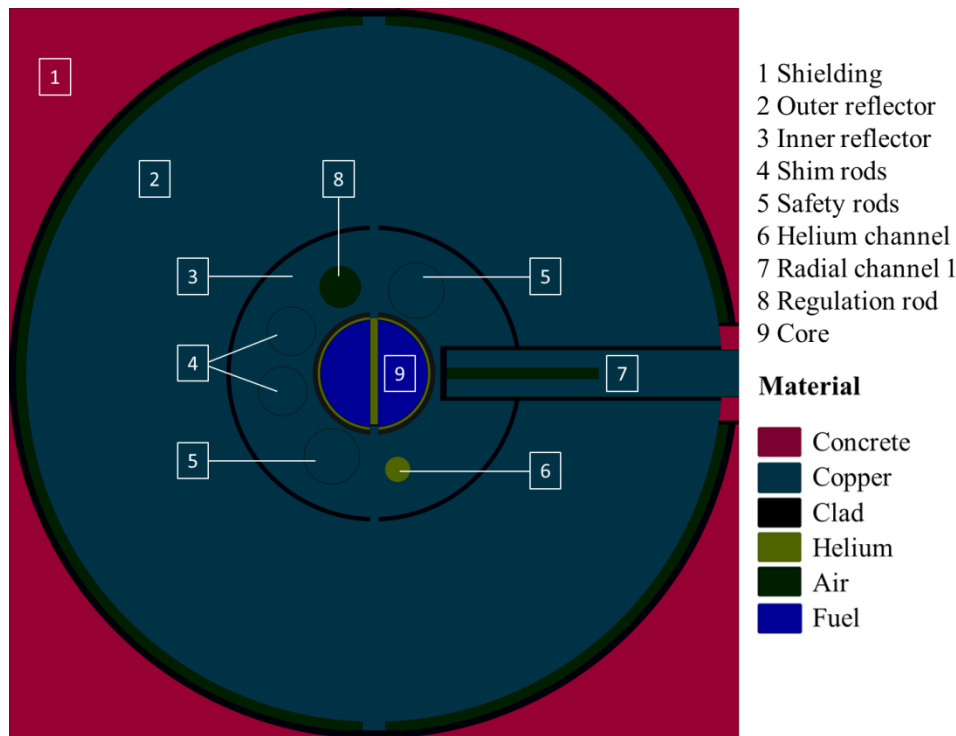


Figure 4 - The TAPIRO reactor model in Serpent: xy-section at $z=0$.

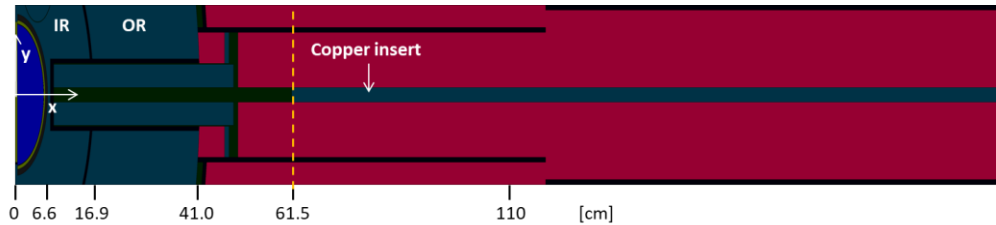


Figure 3 - xy-section of RC1 at $z=0$. The yellow line indicates the position of the copper insert, at a radius of 61.5 cm.

The version of the Serpent code employed in the calculations is distributed with cross-section libraries processed by the developers which are based on JEF-2.2, JEFF-3.1, JEFF-3.1.1, ENDF/B-VI.8 and ENDF/B-VII. In previous evaluations, the material properties have been extracted from the JEFF-3.1.1 library and all the cross section have been taken at 300 K. However, new libraries can be produced from raw ENDF format data using the NJOY nuclear data processing system [15].

From ENDF/B-VIII.beta5 nuclear data (released in October 2017) [12,13] new libraries for Serpent have been generated with NJOY [15], to implement recent data in the TAPIRO model.

To analyse the effect of the new cross section of copper, the results using the following libraries have been compared:

- the library based on JEFF-3.1.1, as already used in previous evaluations;
- a modified version of the JEFF-3.1.1 library, substituting the original files for copper isotopes with the new ACE files for copper made available by the elaboration of the ENDF/B-VIII.beta5 library with NJOY;

- a complete new ENDF/B-VIII.beta5-based library, containing all the newly-generated ACE files.

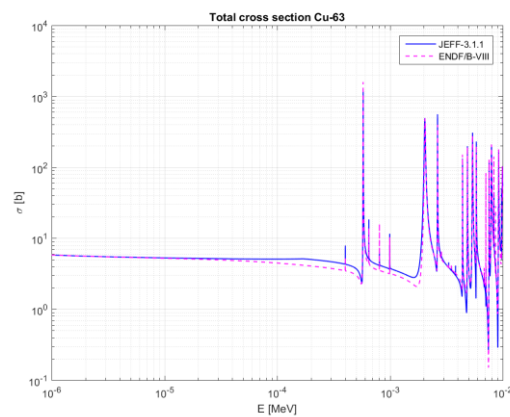
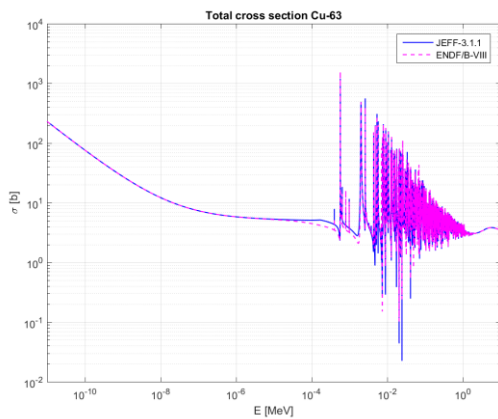
In order to preclude the possibility of introducing additional uncertainty due to the approximations employed in the processing of the data libraries, the same set of options utilised for the libraries distributed with the Serpent code have been adopted to process the ENDF/B-VIII.beta5 nuclear data. The purpose is to compare the experimental fission rates in RC1 with the results of Monte Carlo simulations, to assess the role of the nuclear data, with a specific focus on the role of copper.

4 COMPARISON OF NUCLEAR DATA LIBRARIES

In this section, data and results obtained using different cross section libraries are reported and discussed.

4.1 Copper cross section behavior in JEFF-3.1.1 vs. ENDF/B-VIII

Figures 6 through 8 illustrate the energy dependence of some significant cross sections for the two isotopes considered in the composition of natural copper (69.2% Cu-63 and 30.8% Cu-65). The JEFF-3.1.1 data appear to be higher than the ones in ENDF/B-VIII and, therefore, one can foresee a weaker decay of the neutron flux if the new library is adopted. A further comparison has been performed between the new JEFF library (JEFF-3.2) and ENDF/B-VIII, in which the discrepancies for this data between the two libraries is very small.



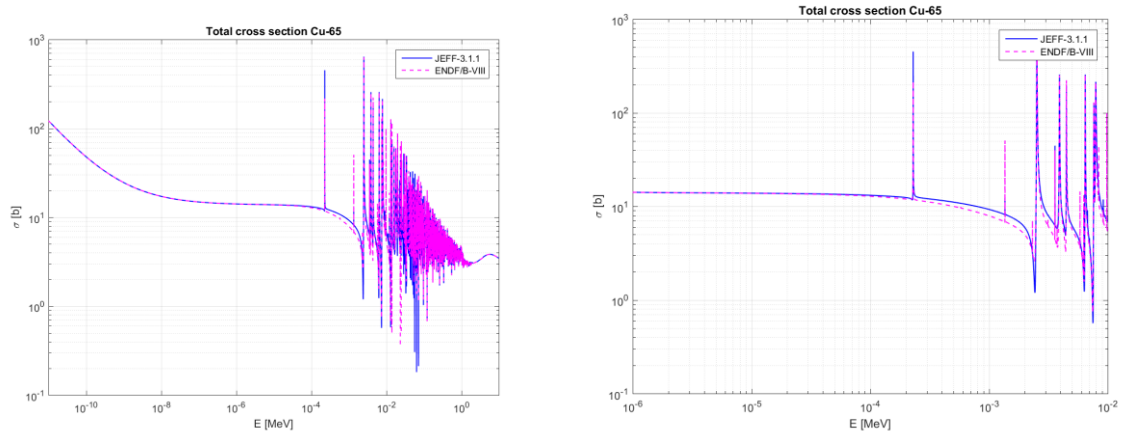


Figure 4 - Comparison of the total cross section data for the two copper isotopes in JEFF-3.1.1 and ENDF/B-VIII. Left graphs: full energy range; right graphs: zoom in range $[10^{-6}; 10^{-2}]$ MeV.

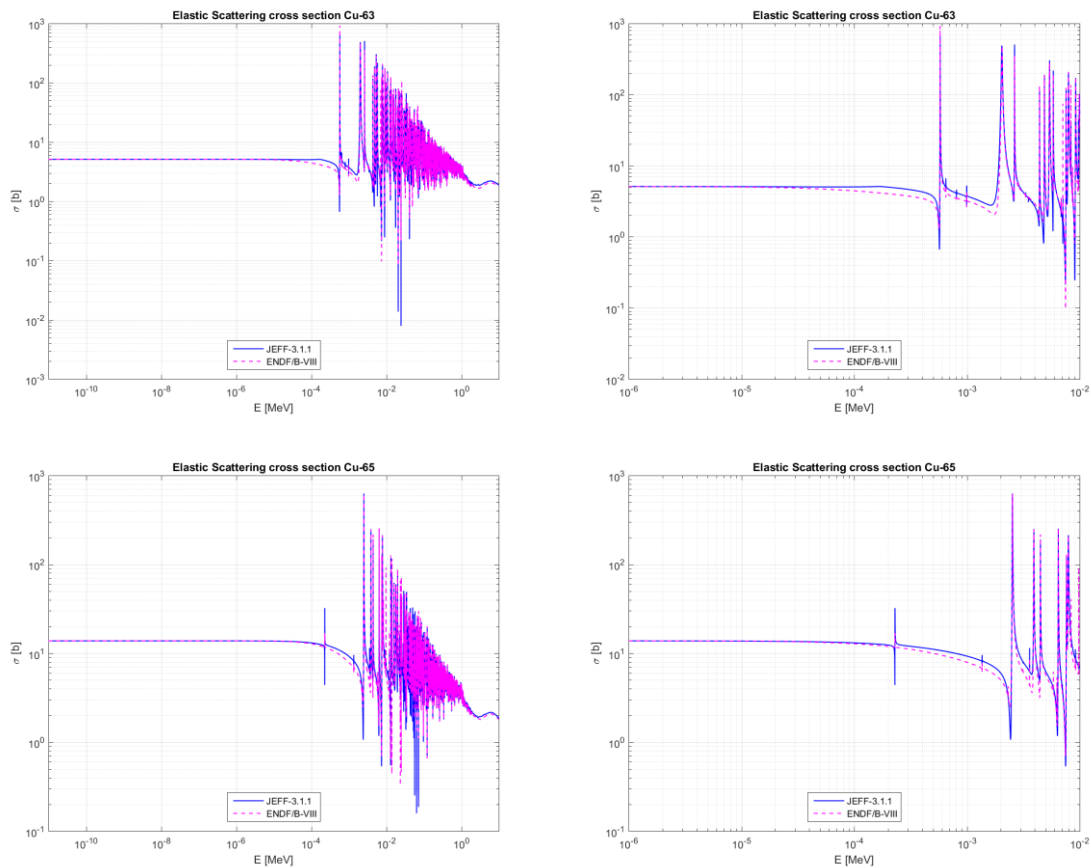


Figure 7 - Comparison of the elastic scattering cross section data for the two copper isotopes in JEFF-3.1.1 and ENDF/B-VIII. Left graphs: full energy range; right graphs: zoom in range $[10^{-6}; 10^{-2}]$ MeV.

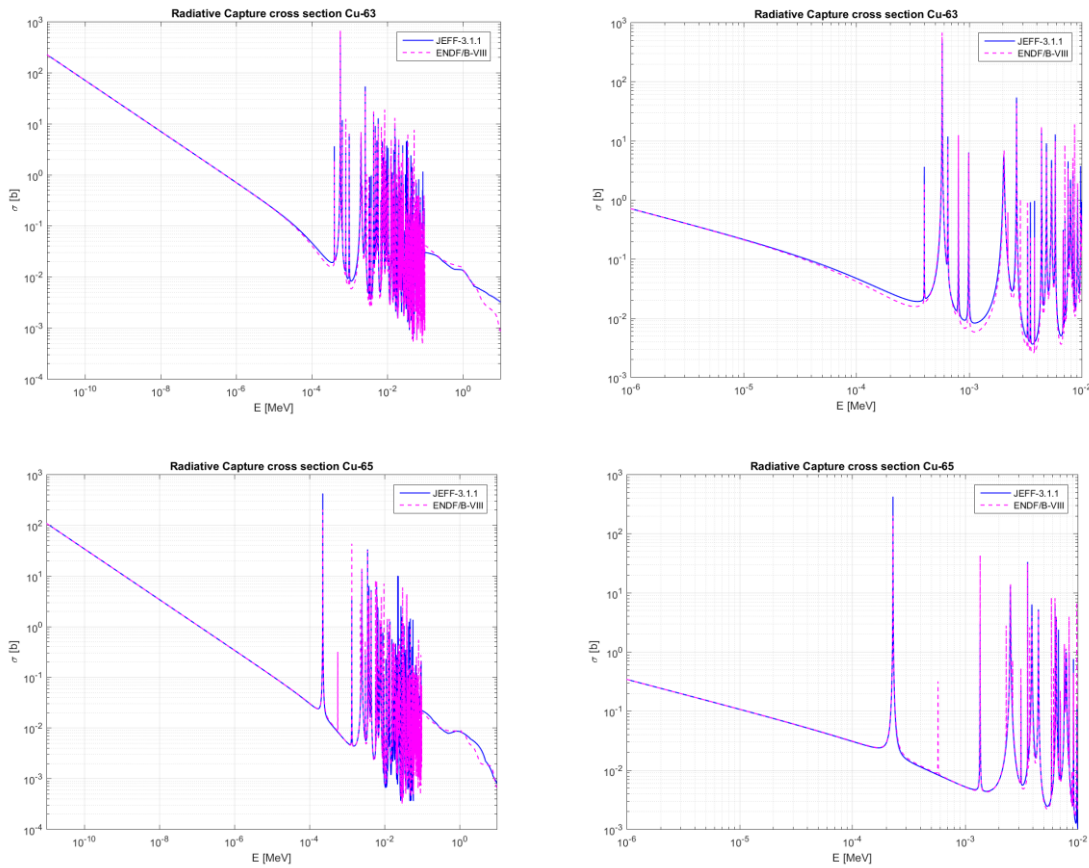


Figure 8 - Comparison of the radiative capture cross section data for the two copper isotopes in JEFF-3.1.1 and ENDF/B-VIII. Left graphs: full energy range; right graphs: zoom in range $[10^{-6}; 10^{-2}]$ MeV.

4.2 Effect of cross section data on the fission rate Monte Carlo estimations

The graphs shown in Fig. 9 report the radial behavior of different fission rates as simulated by Serpent and measured in the experimental campaign. The same results are given in numerical form in Table 1. For the sake of comparison, the reaction rates are normalized to the same spatial integral along the axis of the channel. On one hand, if the new data are only used (JEFFmod results), one can see that the simulated reaction rates are in a better agreement with the experimental values. On the other hand, if the full new library data is used (ENDF/B-VIII results), results are further modified and the agreement may deteriorate depending on the isotope considered. To better appreciate the different effects of library data, the differences between experimental and simulated data are collected in Tables 2-5: a sign disagreement is observed in some locations along the radial coordinate.

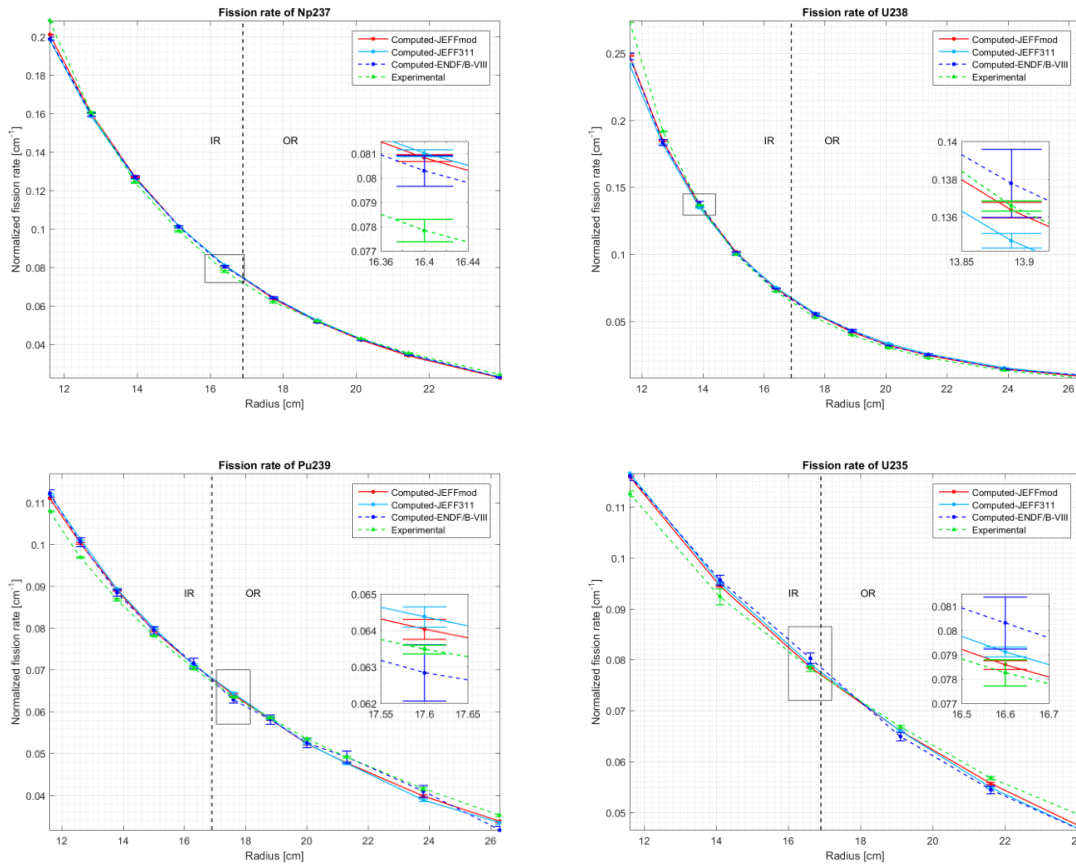


Figure 9 – Comparison of reaction rates (normalized to their spatial integral) in RC1: experimental, and Serpent simulation with the three library options. Same results in table form follow in Table 2.

At last, the multiplication constant of the system is compared in Table 6: the effect is surely non-negligible, especially when focusing on the modification of copper cross sections only.

In order to better investigate the neutronics in the measurement channel, the surface neutron currents evaluated with different libraries are compared in Figs. 10 and 11: the results confirm that the modification of copper nuclear data has a relevant effect, especially in some energy ranges.

Table 1 - Fission rates of Np-237, U-238, Pu-239 and U-235 (normalized to their spatial integral) in RCI with different libraries. The position r [cm] is the distance of the point of measurement from the centre of the core.

r [cm]	Experimental	JEFF-3.1.1	JEFF-3.1.1 mod.	ENDF/B-VIII.beta5
Np-237				
11.60	0.2083 (\pm 9E-04)	0.1984 (\pm 2E-04)	0.2011 (\pm 2E-04)	0.199 (\pm 1E-03)
12.74	0.1605 (\pm 5E-04)	0.1585 (\pm 2E-04)	0.1600 (\pm 2E-04)	0.1596 (\pm 9E-04)
13.94	0.1242 (\pm 4E-04)	0.1262 (\pm 2E-04)	0.1270 (\pm 2E-04)	0.1269 (\pm 8E-04)
15.14	0.0987 (\pm 3E-04)	0.1015 (\pm 2E-04)	0.1016 (\pm 2E-04)	0.1011 (\pm 7E-04)
16.40	0.0778 (\pm 5E-04)	0.0810 (\pm 1E-04)	0.0808 (\pm 1E-04)	0.0803 (\pm 6E-04)
17.74	0.0619 (\pm 4E-04)	0.0641 (\pm 1E-04)	0.0636 (\pm 1E-04)	0.0641 (\pm 5E-04)
18.94	0.05197 (\pm 8E-05)	0.0523 (\pm 1E-04)	0.0517 (\pm 1E-04)	0.0515 (\pm 5E-04)
20.14	0.0428 (\pm 1E-04)	0.0426 (\pm 1E-04)	0.0421 (\pm 1E-04)	0.0424 (\pm 4E-04)
21.44	0.0352 (\pm 3E-04)	0.03441 (\pm 9E-05)	0.03385 (\pm 9E-05)	0.0347 (\pm 4E-04)
23.94	0.02419 (\pm 7E-05)	0.02282 (\pm 7E-05)	0.02242 (\pm 7E-05)	0.0227 (\pm 3E-04)
U-238				
11.59	0.274 (\pm 1E-03)	0.2417 (\pm 5E-04)	0.2485 (\pm 6E-04)	0.248 (\pm 2E-03)
12.69	0.1918 (\pm 2E-04)	0.1818 (\pm 5E-04)	0.1847 (\pm 5E-04)	0.183 (\pm 2E-03)
13.89	0.1366 (\pm 3E-04)	0.1347 (\pm 4E-04)	0.1364 (\pm 4E-04)	0.138 (\pm 2E-03)
15.09	0.0997 (\pm 1E-04)	0.1008 (\pm 3E-04)	0.1016 (\pm 4E-04)	0.101 (\pm 2E-03)
16.39	0.0721 (\pm 1E-04)	0.0751 (\pm 3E-04)	0.0744 (\pm 3E-04)	0.073 (\pm 1E-03)
17.69	0.05274 (\pm 9E-05)	0.0558 (\pm 2E-04)	0.0553 (\pm 3E-04)	0.055 (\pm 1E-03)
18.89	0.03961 (\pm 5E-05)	0.043 (\pm 2E-04)	0.0418 (\pm 2E-04)	0.043 (\pm 1E-03)
20.09	0.0302 (\pm 2E-04)	0.0332 (\pm 2E-04)	0.0321 (\pm 2E-04)	0.0313 (\pm 9E-04)
21.39	0.02256 (\pm 5E-05)	0.0254 (\pm 2E-04)	0.0243 (\pm 2E-04)	0.0250 (\pm 8E-04)
23.89	0.01319 (\pm 6E-05)	0.0152 (\pm 1E-04)	0.0144 (\pm 1E-04)	0.0140 (\pm 6E-04)
26.39	0.00772 (\pm 2E-05)	0.0094 (\pm 1E-04)	0.0088 (\pm 1E-04)	0.0098 (\pm 5E-04)
Pu-239				
11.20	0.1135 (\pm 3E-04)	0.1169 (\pm 2E-04)	0.116 (\pm 2E-04)	0.116 (\pm 9E-04)
11.60	0.1079 (\pm 2E-04)	0.1119 (\pm 2E-04)	0.1111 (\pm 2E-04)	0.1122 (\pm 9E-04)
12.60	0.0969 (\pm 2E-04)	0.1013 (\pm 3E-04)	0.1003 (\pm 2E-04)	0.101 (\pm 1E-03)
13.80	0.0868 (\pm 3E-04)	0.0893 (\pm 2E-04)	0.0891 (\pm 3E-04)	0.0885 (\pm 8E-04)
15.00	0.0781 (\pm 1E-04)	0.08 (\pm 3E-04)	0.0794 (\pm 3E-04)	0.0795 (\pm 9E-04)
16.30	0.0704 (\pm 3E-04)	0.0712 (\pm 2E-04)	0.0712 (\pm 3E-04)	0.072 (\pm 1E-03)
17.60	0.0635 (\pm 1E-04)	0.0644 (\pm 3E-04)	0.064 (\pm 3E-04)	0.0628 (\pm 8E-04)
18.80	0.0585 (\pm 3E-04)	0.0584 (\pm 3E-04)	0.0582 (\pm 3E-04)	0.058 (\pm 1E-03)
20.00	0.0535 (\pm 3E-04)	0.0524 (\pm 3E-04)	0.0523 (\pm 3E-04)	0.053 (\pm 1E-03)
21.30	0.0492 (\pm 2E-04)	0.0476 (\pm 3E-04)	0.0477 (\pm 3E-04)	0.049 (\pm 1E-03)
23.80	0.0416 (\pm 3E-04)	0.0389 (\pm 3E-04)	0.0398 (\pm 3E-04)	0.041 (\pm 1E-03)
26.30	0.0352 (\pm 3E-04)	0.0334 (\pm 3E-04)	0.0338 (\pm 3E-04)	0.0317 (\pm 1E-03)
U-235				
11.60	0.1126 (\pm 6E-04)	0.1166 (\pm 2E-04)	0.1159 (\pm 2E-04)	0.1161 (\pm 9E-04)
14.10	0.092 (\pm 2E-03)	0.0951 (\pm 2E-04)	0.0945 (\pm 2E-04)	0.096 (\pm 1E-03)
16.60	0.0783 (\pm 5E-04)	0.0791 (\pm 2E-04)	0.0786 (\pm 2E-04)	0.080 (\pm 1E-03)
19.10	0.0669 (\pm 3E-04)	0.066 (\pm 2E-04)	0.0660 (\pm 2E-04)	0.0649 (\pm 9E-04)
21.60	0.0568 (\pm 3E-04)	0.0549 (\pm 2E-04)	0.0557 (\pm 2E-04)	0.0545 (\pm 8E-04)
24.10	0.0494 (\pm 5E-04)	0.0466 (\pm 2E-04)	0.0472 (\pm 2E-04)	0.0466 (\pm 8E-04)

Table 2 - Differences between the experimental measurements and the corresponding computed values of the fission rates of Np-237 (normalized to the spatial integral) in RCI

with different libraries. The position r [cm] is the distance of the point of measurement from the centre of the reference frame.

Np-237

r [cm]	JEFF-3.1.1	JEFF-3.1.1 mod.	ENDF/B-VIII.beta5
11.60	0.0099 (9E-04)	0.0072 (9E-04)	0.009 (1E-03)
12.74	0.0020 (5E-04)	0.0005 (5E-04)	0.001 (1E-03)
13.94	-0.0020 (4E-04)	-0.0028 (4E-04)	-0.0027 (9E-04)
15.14	-0.0028 (4E-04)	-0.0029 (4E-04)	-0.0024 (8E-04)
16.40	-0.0032 (5E-04)	-0.0030 (5E-04)	-0.0025 (8E-04)
17.74	-0.0022 (4E-04)	-0.0017 (4E-04)	-0.0022 (7E-04)
18.94	-0.0003 (1E-04)	0.0003 (1E-04)	0.0005 (5E-04)
20.14	0.0002 (1E-04)	0.0007 (1E-04)	0.0004 (5E-04)
21.44	0.0008 (3E-04)	0.0014 (3E-04)	0.0005 (5E-04)
23.94	0.0014 (1E-04)	0.0018 (1E-04)	0.0015 (3E-04)

Table 3 - Differences between the experimental measurements and the corresponding computed values of the fission rates of U-238 (normalized to the spatial integral) in RC1 with different libraries. The position r [cm] is the distance of the point of measurement from the centre of the reference frame.

U-238

r [cm]	JEFF-3.1.1	JEFF-3.1.1 mod.	ENDF/B-VIII.beta5
11.59	0.033 (1E-03)	0.026 (1E-03)	0.027 (3E-03)
12.69	0.0100 (5E-04)	0.0071 (5E-04)	0.008 (2E-03)
13.89	0.0018 (5E-04)	0.0002 (5E-04)	-0.001 (2E-03)
15.09	-0.0012 (4E-04)	-0.0019 (4E-04)	-0.001 (2E-03)
16.39	-0.0030 (3E-04)	-0.0022 (3E-04)	-0.001 (1E-03)
17.69	-0.0031 (3E-04)	-0.0026 (3E-04)	-0.002 (1E-03)
18.89	-0.0033 (2E-04)	-0.0022 (2E-04)	-0.003 (1E-03)
20.09	-0.0030 (3E-04)	-0.0019 (3E-04)	-0.0011 (9E-04)
21.39	-0.0029 (2E-04)	-0.0018 (2E-04)	-0.0025 (8E-04)
23.89	-0.0020 (1E-04)	-0.0012 (1E-04)	-0.0008 (6E-04)
26.39	-0.0017 (1E-04)	-0.0011 (1E-04)	-0.0021 (5E-04)

Table 4 - Differences between the experimental measurements and the corresponding computed values of the fission rates of Pu-239 (normalized to the spatial integral) in RCI with different libraries. The position r [cm] is the distance of the point of measurement from the centre of the reference frame.

Pu-239			
r [cm]	JEFF-3.1.1	JEFF-3.1.1 mod.	ENDF/B-VIII.beta5
11.20	-0.0035 (4E-04)	-0.0025 (4E-04)	-0.0026 (9E-04)
11.60	-0.0040 (3E-04)	-0.0032 (3E-04)	-0.0043 (9E-04)
12.60	-0.0044 (3E-04)	-0.0034 (3E-04)	-0.004 (1E-03)
13.80	-0.0025 (4E-04)	-0.0023 (4E-04)	-0.0016 (8E-04)
15.00	-0.0019 (3E-04)	-0.0013 (3E-04)	-0.0013 (9E-04)
16.30	-0.0008 (4E-04)	-0.0008 (4E-04)	-0.001 (1E-03)
17.60	-0.0009 (3E-04)	-0.0006 (3E-04)	0.0006 (8E-04)
18.80	0.0002 (4E-04)	0.0003 (4E-04)	0.000 (1E-03)
20.00	0.0011 (4E-04)	0.0012 (4E-04)	0.001 (1E-03)
21.30	0.0015 (4E-04)	0.0014 (4E-04)	0.000 (1E-03)
23.80	0.0027 (4E-04)	0.0018 (5E-04)	0.001 (1E-03)
26.30	0.0018 (4E-04)	0.0014 (4E-04)	0.003 (1E-03)

Table 5 - Differences between the experimental measurements and the corresponding computed values of the fission rates of U-235 (normalized to the spatial integral) in RCI with different libraries. The position r [cm] is the distance of the point of measurement from the centre of the reference frame.

U-238			
r [cm]	JEFF-3.1.1	JEFF-3.1.1 mod.	ENDF/B-VIII.beta5
11.60	-0.0039 (6E-04)	-0.0033 (6E-04)	-0.004 (1E-03)
14.10	-0.003 (2E-03)	-0.002 (2E-03)	-0.003 (2E-03)
16.60	-0.0009 (6E-04)	-0.0003 (6E-04)	-0.002 (1E-03)
19.10	0.0008 (3E-04)	0.0008 (3E-04)	0.0019 (9E-04)
21.60	0.0019 (3E-04)	0.0011 (3E-04)	0.0023 (8E-04)
24.10	0.0028 (5E-04)	0.0022 (5E-04)	0.0028 (9E-04)

Table 6 - Monte Carlo estimate of k_{eff} for the complete geometry model of the TAPIRO reactor (copper plug in RCI inserted at the inner position) and with different nuclear data libraries.

	JEFF-3.1.1	JEFF-3.1.1 mod.	ENDF/B-VIII.beta5
k_{eff}	1.00787 ($\pm 6.5E-06$)	1.00309 ($\pm 6.5E-06$)	1.00594 ($\pm 2.9E-05$)

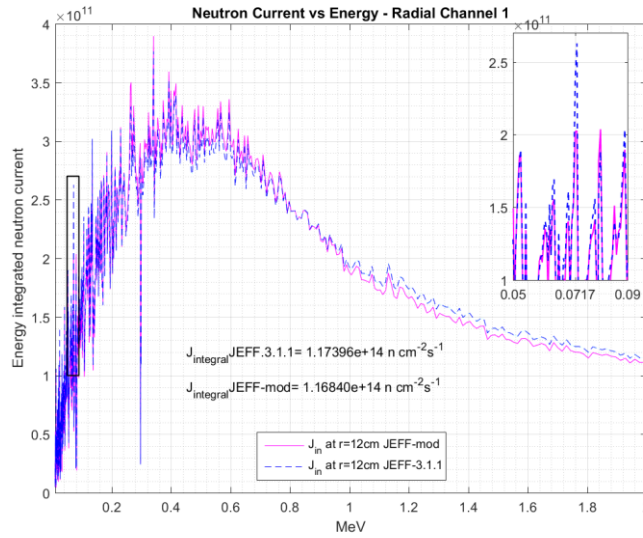


Figure 10 – Neutron current (as function of energy) entering RC1 at 12 cm distance from the system center, estimated with the JEFF-3.1.1 and the JEFF-3.1.1-modified libraries. The zoom shows a detail of the resonance region. The maximum relative standard deviation of the estimates is 0.4472 (at very low energy, owing to the poor statistics) while the average is 0.0049. The integral of the current over the entire energy range is also reported.

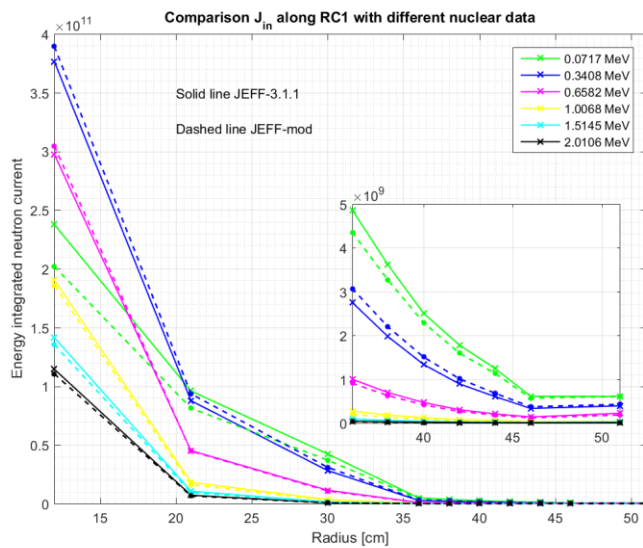



Figure 11 – Spatial distribution along the RC1 axis of the entering current at different energies, estimated with the JEFF-3.1.1 and the JEFF-3.1.1 modified libraries.

 Ricerca Sistema Elettrico	Sigla di identificazione	Rev.	Distrib.	Pag.	di
	ADPFISS – LP2 – 157	0	L	16	17


5 CONCLUSIONS

The comparison between measured and simulated values of some reaction rates in the TAPIRO reactor allow an assessment of the effect of different cross section libraries. In particular, the data for copper play an important role in this experimental facility. The results presented show that the adoption of new nuclear data libraries leads to significantly different results. However, such adoption does not always lead to an improvement of the quality of the simulations as compared to the experimental measurements in TAPIRO. Further work is needed to draw a definite conclusion on the appropriateness of the new cross section data.

In this perspective, performing a sensitivity analysis of the MA reaction rates as a function of the nuclear data, evidencing the relative role of each components, should be envisaged. This activity is foreseen as future work.

6 LIST OF REFERENCES

1. “Nuclear Energy Agency, Expert Group on Integral Experiments for Minor Actinide Management section.” (2017). URL <https://www.oecd-nea.org/science/ma/>.
2. “ENEA, TAPIRO.” (2017). URL <http://www.enea.it/en/research-development/documents/nuclear-fission/tapiro-eng-pdf>.
3. C. Bethaz, F. Boccia, M. Carta, P. C. Camprini, V. Fabrizio, O. Fiorani, A. Gandini, A. Grossi, V. Peluso, P. Ravetto, and A. Santagata. “TAPIRO: feasibility study of minor actinides irradiation campaign.” ENEA report ADPFISS-LP2-083, ENEA-CIRTEN (2015).
4. D. Caron, M. Carta, S. Dulla, V. Fabrizio, A. Grossi, V. Peluso, and P. Ravetto. “Assessment of a cross section adjustment formalism using experimental data from the TAPIRO reactor.” ENEA report ADPFISS-LP2-116, ENEA-CIRTEN (2016).
5. Y. Ronen. Uncertainty analysis. CRC Press, Boca Raton (2000).
6. G. Rimpault, D. Plisson, J. Tommasi, R. Jacqmin, J.-M. Rieunier, D. Verrier, and D. Biron. “The ERANOS code and data system for fast reactor neutronic analyses.” In International Conference PHYSOR 2002. Seoul, Korea (2002).
7. X-5 Monte Carlo Team. “MCNP: A General Monte Carlo Transport Code.” LA-CP-03-245, LANL (2003).
8. J. Leppanen, M. Pusa, T. Viitanen, V. Valtavirta, and T. Kaltiaisenaho. “The Serpent Monte Carlo code: Status, development and applications in 2013.” *Annals of Nuclear Energy*, volume 82, pp. 142–150 (2015).
9. O. Dicuonzo, V. Fabrizio, D. Caron, S. Dulla, M. Carta, and P. Ravetto. “Computational Analysis of TAPIRO Experiments by the SERPENT and ERANOS Codes.” In International Conference M&C 2017. Jeju Island, South Korea (2017).

 Ricerca Sistema Elettrico	Sigla di identificazione	Rev.	Distrib.	Pag.	di
	ADPFISS – LP2 – 157	0	L	17	17

10. M. Carta, K. W. Burn, P. C. Camprini, V. Fabrizio, D. Caron, O. Dicuonzo, S. Dulla, and P. Ravetto. “Feasibility studies of an experimental campaign in TAPIRO devoted to the analysis of nuclear database for minor actinides.” ENEA report ADPFISS-LP2-142, ENEA-CIRTEN (2017).
11. A. Santamarina, D. Bernard, P. Blaise, M. Coste, A. Courcelle, T. Huynh, C. Jouanne, P. Leconte, O. Litaize, S. Mengelle, G. Nogue, J.-M. Ruggiri, O. Srot, J. Tommasi, C. Vaglio, and J.-F. Vidal. “The JEFF-3.1.1 nuclear data library (JEFF report 22).” Technical Report NEA No. 6807, Nuclear Energy Agency, Paris (2009).
12. D. Brown and CSEWG. “Preparing for ENDF/B-VIII.” BNL-113667-2017-CP, Brookhaven National Laboratory, Upton, NY (2017).
13. “ENDF/B-VIII, US Library of Evaluated Nuclear Reaction Data.” (2017). URL <https://ndclx4.bnl.gov/gf/project/endl/>.
14. A. Fabry, M. Angelone, H. A. Abderrahim, M. Carta, P. DHondt, S. D. Leeuw, G. D. Leeuw-Gierts, G. Minsart, and P. Moioli. “Learning’s from a joint Italian-Belgium neutronic characterization of the TAPIRO source reactor.” In ASTM-EURATOM Symposium on Reactor Dosimetry. Strasbourg, France (1990).
15. R. E. MacFarlane, D. W. Muir, R. M. Boicourt, A. C. Kahler, and J. L. Conlin. “The NJOY Nuclear Data Processing System.” Version 2016, Los Alamos National Laboratory, Los alamos, NM (2016).